ChemComm

COMMUNICATION

Potential-controlled electrodeposition of gold dendrites in the presence of cysteine†

Tai-Hsuan Lin,[a] **Ching-Wei Lin,**[a] **Hao-Heng Liu,**[b] **Jeng-Tzong Sheu**[b] **and Wei-Hsiu Hung**[*a]

Crystalline Au dendrites were formed by electrodeposition on a glassy carbon electrode from a solution of HAuCl$_4$ containing cysteine. The Au dendrites possessed a hierarchical architecture with three-fold symmetry; they comprised trunks, branches, and nanorod leaves, which all grew along the $\langle 111 \rangle$ direction.

Gold (Au) nanostructures have attracted much attention because their chemical and physical properties differ considerably from those of bulk Au. The flurry of research activity into nanosized Au has been stimulated by its diverse range of prospective applications. For example, the nano-structured Au electrodes exhibit a strong catalytic activity for the oxidation of CO and CH$_3$OH and the reduction of O$_2$.[1] Because the chemical and physical properties of Au nanostructures depend markedly on their sizes and shapes, these properties are tunable through control of morphology and structure.[2] Various chemical methods have been developed for the manufacture of Au nanomaterials possessing various shapes and structures.[3] Much attention has also been paid to the fabrication of the dendrites because of their importance in realizing and understanding the mechanism of growth and their potential applications in catalysis, molecular sensing and other technological fields.[4] In particular, the synthesis of hierarchical architectures in an effective condition, which is an essential step toward merging the nanoscale building blocks into complex functional devices, remains a challenge. Dendritic nanomaterials have been prepared by electrochemical deposition because of its ease of control, highly pure and uniform deposits, and simple operation,[5] but the dendritic Au nanostructure formed from this electrochemical deposition has not been reported. We report here an electrochemical deposition of three-dimensional dendritic Au at 295 K, which is grown simply and rapidly in an aqueous solution; this method is superior to ionic liquid- and surfactant-assisted growths.[6]

The SH groups of thiols adsorb covalently onto Au surfaces to form protecting or insulating layers stabilized through strong Au–S bonds.[7] Such adsorbed thiols can be desorbed through electrochemical reactions at a potential depending on the crystallographic facet of the Au surface. Ohsaka *et al.* demonstrated that cysteine (HO$_2$CCH(NH$_2$)CH$_2$SH) molecules adsorbed on a polycrystalline Au (poly-Au) electrode were removed selectively from domains presenting plane (111), but remained on domains presenting planes (110) and (100), during a potential-controlled reductive desorption.[8] In this communication, we report the induction of anisotropic crystal growth of Au after an addition of cysteine to an electrochemical solution; controlling the potential of deposition resulted in the formation of Au dendrites on a glassy carbon (GC) surface.

Reduction of Au^{3+} ion resulted in deposition of the Au metal on GC from a HAuCl$_4$ solution at a potential less than $\sim +0.8$ V (*vs.* SCE), according to a cyclic voltammetric (CV) scan (Fig. S1, ESI†). The cysteine adsorbed on the poly-Au was removable from Au(111) domains at a potential in a range between -0.7 and -0.9 V through reductive desorption but remained on Au(100) and (110) (Fig. S2, ESI†). The reduction of Au^{3+} to form Au is thus expected to occur preferentially on Au(111) facets on a poly-Au surface in HAuCl$_4$ solution containing cysteine at -0.8 V, because cysteine adsorbed on Au(100) and (110) acts as a blocking molecule. The presence of cysteine in the solution of HAuCl$_4$ might induce anisotropic growth during electrodeposition.

Fig. 1 displays SEM images of the Au structures electrodeposited onto a GC electrode in HAuCl$_4$ solutions in the absence and presence of cysteine. In the absence of cysteine, the deposited Au possessed a structure of densely packed nanoparticles, as previously reported.[9] The growth rate of
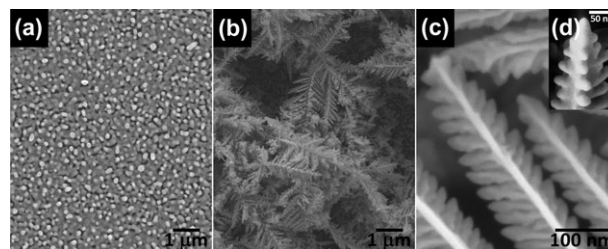
[a] *Department of Chemistry, National Taiwan Normal University, 88, Sec.4, Ting-Chow Road, Taipei 116, Taiwan.*
E-mail: whung@ntnu.edu.tw; Fax: 011-886-29324249;
Tel: 011-886-77346125
[b] *Institute of Nanotechnology, National Chiao-Tung University, Hsinchu, 300, Taiwan*

Fig. 1 SEM images of Au structures electrodeposited onto a GC electrode from a solution of 1.0 mM HAuCl$_4$ and 0.5 M H$_2$SO$_4$ in the (a) absence and (b) presence of 0.1 mM cysteine for 3000 s. (c) and (d) Highly magnified SEM images of the Au dendrites in (b).

Au was isotropic during electrodeposition. This indicated that the deposition rate was rapid and independent of the crystallographic direction in a solution. The deposited Au did not show any preferential growth along a specific crystallographic direction. In contrast, we obtained a hyperbranched Au dendrite in the presence of cysteine. The magnified SEM images in Fig. 1(c) and (d) indicate that the Au dendrite possessed a hierarchical structure with three-fold symmetry. The presence of cysteine in solution thus had a considerable effect on the shape and structure of the electrodeposited Au. The stems and branches of Au dendrites are oriented with no preferential direction normal to the electrode; this behaviour is different from that expected if the formation of dendritic Au is due to the diffusion limit.[10]

The XRD measurement indicated that these Au dendrites have a face-centered cubic (fcc) lattice (Fig. S3, ESI†). The sharp diffraction features indicate that the Au dendrites were highly crystalline. The ratios of the intensities at the peaks due to the (111) plane relative to the (200) and (220) planes were 3.1 and 5.9, respectively; these values are significantly greater than those (1.9 and 3.1, respectively) commonly obtained for poly-Au (JCPDS 04-0784). These observations suggest that the (111) plane was the predominant orientation in the Au dendrites, which grew preferentially along the $\langle 111 \rangle$ direction. In addition, the EDX spectrum of the dendrites reveals characteristic peaks corresponding to the Au metal (Fig. S4, ESI†). The only other major signal was a small one at *ca.* 280 eV, due to carbon atoms, originating from the underlying GC electrode. Therefore, the EDX spectrum confirmed that the dendrites were essentially composed of highly pure Au metal.

The crystal orientation and growth direction of Au dendrites were determined with measurements on a transmission electron microscope (TEM). Fig. 2(a) shows the TEM image of an Au 'sprout' dendrite that has just begun to grow branches, which enables an examination of the growth direction of the dendrite. The electron-diffraction pattern of a selected area (SAED) and high-resolution TEM (HRTEM) images were recorded at the thin tips of the trunk and the short branch, at which the reaction of $HAuCl_4$ to form Au is expected to occur and to grow the dendritic structure. The SAED pattern of the trunk tip exhibits clear diffraction spots indexed to the [112] zone axis of the fcc Au single crystal, indicating that the initially grown Au dendrites are single-crystalline with the trunk grown along the $\langle 111 \rangle$ direction. HRTEM measurements also demonstrated this single-crystalline nature of the Au dendrite at the tip areas of the trunk and branch as seen in Fig. 2(b) and (c). The atomic lattice exhibits a *d*-spacing of 2.4 Å at the axial direction of the trunk and branch, identical to the *d*-spacing of (111) planes for the fcc Au crystal.

The growth direction of Au is further confirmed by recording the TEM image of a two-generation Au dendrite, as shown in Fig. 2(d). The dendrite comprises three groups of parallel branches on the main trunk; two groups extend downward and one group extends right above the trunk. The angles between these groups of branches and the trunk in the image are typically ~ 65–$70°$, near the theoretical angle $67.8°$ between two $\langle 111 \rangle$ directions of the fcc structure in the $(11\bar{2})$ projection plane as shown in Fig. S5 (ESI†). Thus, the combined results from TEM and ED indicate that the trunk and branches of an Au dendrite constitute a single crystal grown along the $\langle 111 \rangle$ direction.

The CV scans of the as-grown Au dendrite on the GC electrode in 0.5 M KOH show a broad cathodic feature that appeared at -1.04 V with a shoulder at -1.16 V, consistent with the reductive desorption of cysteine from the Au(100) and (110) surfaces (Fig. S6, ESI†).[8] This indicates that cysteine molecules had adsorbed onto the (100) and (110) facets of the Au dendrites during electrodeposition. To examine further the facets present on the Au dendrites, we immersed a Au dendrite-deposited GC electrode in a solution of 1.0 mM cysteine for 15 min to ensure the formation of a monolayer of cysteine over all of the facets of the Au dendrites. The resulting CV scans of the dendrite-deposited GC electrode after treatment with the cysteine solution show an additional and intense cathodic feature that appeared at -0.73 V, which we attribute to the reductive desorption of cysteine from the Au(111) facet, as previously reported.[7] The domains of all three facets—(100), (110), and (111)—existed on the surfaces of the Au dendrites during electrodeposition. At -0.80 V, the (111) facet remained free of cysteine and was available for the deposition of Au; in contrast, cysteine remained adsorbed on the (100) and (110) facets, hindering the deposition of Au.[11] The adsorbed cysteine molecules on facets (100) and (110) increased the interfacial resistance between the surface and the solution, acting as blocking molecules for the reduction of $HAuCl_4$. The preferential deposition of Au on facet (111) resulted in formation of the dendritic structure.

Fig. 3 presents a schematic representation of the proposed mechanism for Au dendrite growth in a $HAuCl_4$ solution containing cysteine. Initially, Au nanoparticles formed with crystallographic (111), (110), and (100) facets gradually developing on the surfaces of the incipient Au nanoparticles. A layer of cysteine would form on each Au nanoparticle during the electrodeposition, thereby increasing the surface resistance and reducing the electrochemical activity of the Au surface significantly. The cysteine molecules adsorbed on the (111)
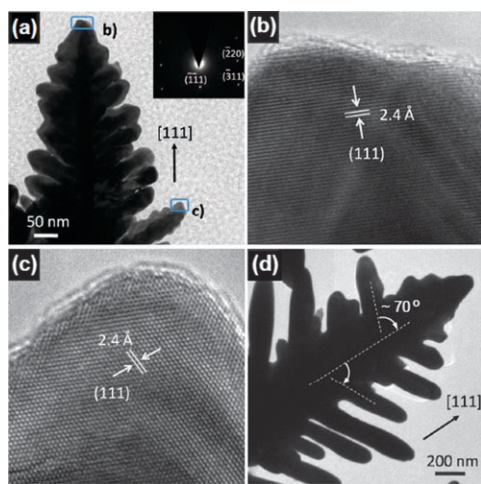

Fig. 2 (a) TEM image of an Au sprout (inset: SAED pattern of the Au sprout). (b) and (c) HRTEM images of the tips of the trunk and branch marked in (a). (d) TEM image of the two-generation Au dendrite.
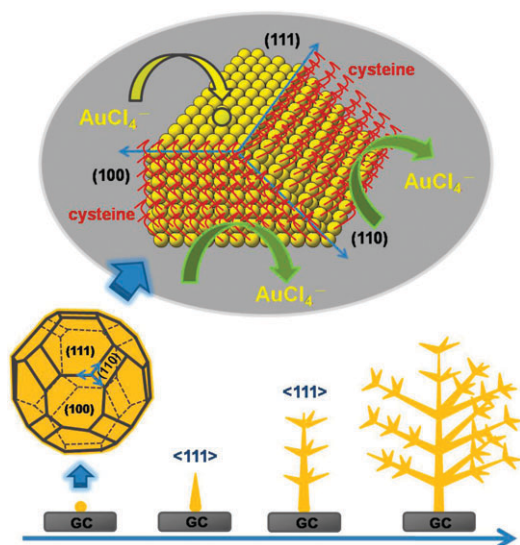
Fig. 3 Schematic representation of the proposed mechanism of formation of dendritic Au.

facet were removed selectively when the applied potential is at the range between −0.7 and −0.9 V. In this study, the (111) facet is free of cysteine at a potential of −0.8 V and is thus directly exposed to the solution, whereas the (100) and (110) facets remained covered with cysteine. The electrodeposition of Au thus occurs preferentially along on the ⟨111⟩ direction and eventually forms the three-fold dendritic structure.

The shapes and morphologies of nano-structured crystals or polycrystals are greatly affected by the driving force of crystallization and the rate of diffusion of the reactants.[10] The branched and dendritic structure is expected to form under the growth condition of the diffusion limit, but we propose that we formed dendritic Au because of selective desorption of cysteine adsorbed on the (111) facets. We tested other compounds including 4-mercaptobenzoic acid ($HOOCC_6H_4SH$) and alkanethiols with alkyl chains of varied length. The dendrites were also obtained in the presence of various molecules which differ in the extent of structural morphology and symmetry (Fig. S7, ESI†). The Au dendrite was not formed at the high concentrations of additive compounds because the surface was mostly adsorbed and the deposition growth of Au was greatly inhibited.

Electro-oxidation of CH_3OH is commonly used to evaluate the catalytic activity of nanostructured Au. Before the CV measurement, the Au dendrite as grown on GC was pretreated at potential −1.2 V to remove all cysteine adsorbed on the surface. The CV measurements of an Au-dendrite-deposited GC electrode in an alkaline solution of CH_3OH show an anodic peak at 0.26 V, which is less positive than that on the poly-Au electrode by 0.05 V (Fig. S8, ESI†). This signal is ascribed to the electro-oxidation of CH_3OH to formate via a reaction involving a four-electron transfer. As a measure of catalytic activity, the current density of oxidation on the Au-dendrite-deposited electrode is 110.0 µA cm^{-2}, approximately five times that (26.6 µA cm^{-2}) on the poly-Au electrode. The negative shift of the oxidation potential and the enhanced current density are responsible for the catalytic effect of the Au dendrite towards electro-oxidation of methanol. The

hyperbranched Au dendrite with the nanosized structure is likely rich in active sites (e.g. kink or step sites) on the surface and thus exhibits a high electrocatalytic activity. The Au dendrites electrodeposited at varied potentials result in an altered proportion of area of Au(111) on the surface of the dendrites, which also affects significantly the catalytic activity.

In conclusion, our approach for the synthesis of nano-structured Au dendrites is based on the selective adsorption and desorption of a blocking molecule (cysteine) under a controlled electrochemical potential. The hyperbranched Au dendrites were obtained on a GC electrode through electrodeposition from a solution of $HAuCl_4$ containing cysteine, under a square-wave potential. The crystalline Au grew preferentially along the ⟨111⟩ direction and exhibited a three-fold symmetric hierarchy. This strategy of selective desorption via an appropriately chosen blocking molecule under a suitable deposition potential might be applicable to the fabrication of other nano-structured materials.

Notes and references

1 (a) B. R. Cuenya, S.-H. Baeck, T. F. Jaramillo and E. W. McFarland, *J. Am. Chem. Soc.*, 2003, **125**, 12928; (b) M. M. Maye, Y. Lou and C.-J. Zhong, *Langmuir*, 2000, **16**, 7520; (c) B. K. Jena and C. R. Raj, *Langmuir*, 2007, **23**, 4064; (d) M.-C. Daniel and D. Astru, *Chem. Rev.*, 2004, **104**, 293; (e) M. S. El-Deab and T. Ohsaka, *Electrochem. Commun.*, 2002, **4**, 288.

2 (a) F. Jackel, A. A. Kinkhabwala and W. E. Moerner, *Chem. Phys. Lett.*, 2007, **446**, 339; (b) H.-L. Wu, C.-H. Chen and M. H. Huang, *Chem. Mater.*, 2009, **21**, 110; (c) N. Zhao, Y. Wei, N. Sun, Q. Chen, J. Bai, L. Zhou, Y. Qin, M. Li and L. Qi, *Langmuir*, 2008, **24**, 991.

3 (a) R. Bardhan, O. Neumann, N. Mirin, H. Wang and N. J. Halas, *ACS Nano*, 2009, **3**, 266; (b) H.-L. Wu, C.-H. Chen and M.-H. Huang, *Chem. Mater.*, 2009, **21**, 110; (c) C.-C. Chang, H.-L. Wu, C.-H. Kuo and M.-H. Huang, *Chem. Mater.*, 2008, **20**, 7570; (d) T. H. Ha, H.-J. Koo and B. H. Chung, *J. Phys. Chem. C*, 2007, **111**, 1123; (e) J. Xie, J. Y. Lee and D. I. C. Wang, *J. Phys. Chem. C*, 2007, **111**, 10226; (f) J. Hernandez, J. Solla-Gullon, E. Herrero, A. Aldaz and J. M. Feliu, *J. Phys. Chem. B*, 2005, **109**, 12651; (g) C. J. Murphy, T. K. Sau, A. M. Gole, C. J. Orendorff, J. Gao, L. Gou, S. E. Hunyadi and T. Li, *J. Phys. Chem. B*, 2005, **109**, 13857.

4 (a) B. Lim, M. Jiang, P. H. C. Camargo, E. C. Cho, J. Tao, X. Lu, Y. Zhu and Y. Xia, *Science*, 2009, **324**, 1302; (b) X. Wen, Y.-T. Xie, W. C. Mak, K. Y. Cheung, X.-Y. Li, R. Renneberg and S. Yang, *Langmuir*, 2006, **22**, 4836; (c) R. Qiu, X. L. Zhang, R. Qiao, Y. Li, Y. I. Kim and Y. S. Kang, *Chem. Mater.*, 2007, **19**, 4174.

5 (a) Y. J. Song, J. Y. Kim and K. W. Park, *Cryst. Growth Des.*, 2009, **9**, 505; (b) M. N. Nadagouda, M. Schock, D. H. Metz, M. K. DeSantis, D. Lytle and M. Welch, *Cryst. Growth Des.*, 2009, **9**, 1798.

6 (a) Y. Qin, Y. Song, N. Su, N. Zhao, M. Li and L. Qi, *Chem. Mater.*, 2008, **20**, 3965; (b) T. Huang, F. Meng and L. Qi, *Langmuir*, 2010, **26**, 7582.

7 (a) L. H. Dubois and R. G. Nuzzo, *Annu. Rev. Phys. Chem.*, 1992, **43**, 437; (b) A. Ulman, *Chem. Rev.*, 1996, **96**, 1533.

8 (a) M. S. El-Deab, K. Arihara and T. Ohsaka, *J. Electrochem. Soc.*, 2004, **151**, E213; (b) K. Arihara, T. Ariga, N. Takashima, K. Arihara, T. Okajima, F. Kitamura, K. Tokuda and T. Ohsaka, *Phys. Chem. Chem. Phys.*, 2003, **5**, 3758.

9 (a) X. Dai, O. Nekrassova, M. E. Hyde and R. G. Compton, *Anal. Chem.*, 2004, **76**, 5924; (b) F. Gao, M. S. El-Deab, T. Okajima and T. Ohsaka, *J. Electrochem. Soc.*, 2005, **152**, A1226.

10 H. Imai, *Top. Curr. Chem.*, 2007, **270**, 43.

11 (a) M. S. El-Deab, T. Okajima and T. Ohsaka, *J. Electrochem. Soc.*, 2003, **150**, A851; (b) E. R. Vago, K. de Weldige, M. Rohwerder and M. Stratmnann, *Fresenius' J. Anal. Chem.*, 1995, **353**, 316; (c) M. S. El-Deaband and T. Ohsaka, *Electrochem. Commun.*, 2003, **5**, 214.